Scripta Materialia 125 (2016) 29–33

Contents lists available at ScienceDirect

Scripta Materialia

journal homepage: www.elsevier.com/locate/scriptamat

Regular Article

# Platelets-induced stiffening and strengthening of ice-templated highly porous alumina scaffolds

Dipankar Ghosh *, Mahesh Banda, Hyungsuk Kang, Nikhil Dhavale

*Department of Mechanical and Aerospace Engineering, Old Dominion University, Norfolk, VA 23529, USA*

ARTICLE INFO

*Article history:*
Received 30 May 2016
Received in revised form 27 July 2016
Accepted 28 July 2016
Available online xxxx

*Keywords:*
Grain morphology
Freeze casting
Porosity
Interlamellae bridging
Compressive strength

ABSTRACT

This paper describes the effects of the grain-level anisotropy on the microstructure and uniaxial compressive response of the ice-templated alumina scaffolds. Highly porous (~80 vol.%) scaffolds were fabricated from alumina powders of equiaxed morphology as well as from powder mixtures containing equiaxed and small amount of platelet particles. Presence of the platelets (diameter 8 μm and thickness 400 nm) led to the formation of the interlamellae bridges, and significantly enhanced the stiffness and compressive strength of the scaffolds. Measured improvement of the mechanical response is rationalized based on the stiffening and strengthening effects exhibited by the intralamella and interlamella platelets.



Ice-templated anisotropic porous scaffolds can exhibit greater compressive strength relative to the isotropic cellular solids; however, the strength becomes comparable for porosity above 75 vol.% [1,2]. For the ice-templated scaffolds, rate of freezing, suspension viscosity and pH can be varied to increase the interlamellae bridge density and decrease the pore size for the strength enhancement [2–7]. However, such modifications exploiting the above processing variables may not result in an adequate strength improvement for porosity beyond 75 vol.%. Therefore, it is of significant interests to explore the effects of other variables such as the powder particle morphology on the compressive response of ice-templated anisotropic porous ceramics. It may be possible to improve the mechanical response by incorporating grains of anisotropic morphology within the ice-templated porous ceramic scaffold that primarily consist of the equiaxed grains. To this end, we processed ice-templated alumina ($Al_2O_3$) scaffolds from the equiaxed powder particles as well as from the mixtures of the equiaxed and platelet-shaped particles, and investigated the effects of the induced grain-level anisotropy through platelets addition on the uniaxial compressive response. Overall this manuscript aims to shed light on the effects of the grain morphology on the structure-property (mechanical) relationships of the highly porous (~80 vol.%) ice-templated sintered ceramic scaffolds.

$Al_2O_3$ powders of equiaxed morphology of two different sizes (0.3 and 0.9 μm) and of platelet morphology (diameter ~ 8 μm and thickness ~ 400 nm) were utilized; referred to here as NA (nano $Al_2O_3$) for the 0.3 μm particle size, SA (submicron $Al_2O_3$) for the 0.9 μm powder particle size, and PA for the $Al_2O_3$ platelets. Scaffolds were processed from the aqueous suspensions of: (i) NA, (ii) SA, (iii) 90–10 vol.% mixture of NA and PA, and (iv) 90–10 vol.% mixture of SA and PA. For each suspension, total $Al_2O_3$ content was 15 vol.% (details of suspension preparation in Supplementary material). Employing a custom-made freeze casting device, $Al_2O_3$ ceramics were processed within a freezing front velocity (FFV) range of 10–35 μm/s. Frozen samples were freeze-dried at 0.014 mbar pressure and −50 °C for 96 h, and sintered at 1550 °C for 4 h. Microstructures of the porous ceramics were characterized from two different planes located at 5 mm (referred to as bottom plane) and 30 mm (referred to as top plane) heights from the bottom of a sample (Fig. S1a). For each sintered scaffold three specimens were extracted from three specific heights (referred to as #1, #2 and #3, Fig. S1b) and uniaxially compressed in the direction of ice growth at a displacement rate of 0.5 mm/min (Tinius Olsen, 10ST). Specimen dimensions of 8 mm × 8 mm × 4 mm were utilized with 8 mm × 8 mm being the loading surface. Sintered density ($\rho^*$) was determined from the mass and dimensions, and relative density ($\rho_r$) was estimated using $\rho_r = \rho^*/\rho_s$, where $\rho_s$ is the bulk density of $\alpha$-$Al_2O_3$ (3.96 g/cm$^3$).

Fig. 1 shows representative SEM micrographs of both the top and bottom planes of the SA, NA, SA-10PA, and NA-10PA porous (sintered) scaffolds processed at relatively low and high FFVs. Pore morphology of the scaffolds is observed to be primarily lamellar; however, some differences are observed in terms of the extent of the interlamellae bridging. Both the SA (Fig. 1a) and NA (Fig. 1c) porous scaffolds exhibit negligible bridging at low FFVs but an increase of the bridge density is observed at relatively high FFVs (Figs. 1e and g). Both the SA-10PA and NA-10PA scaffolds exhibit relatively higher bridge density both at the relatively low (Figs. 1b and d) and high (Figs. 1f and h) FFVs relative

* Corresponding author.
*E-mail address:* dghosh@odu.edu (D. Ghosh).

http://dx.doi.org/10.1016/j.scriptamat.2016.07.030
1359-6462/

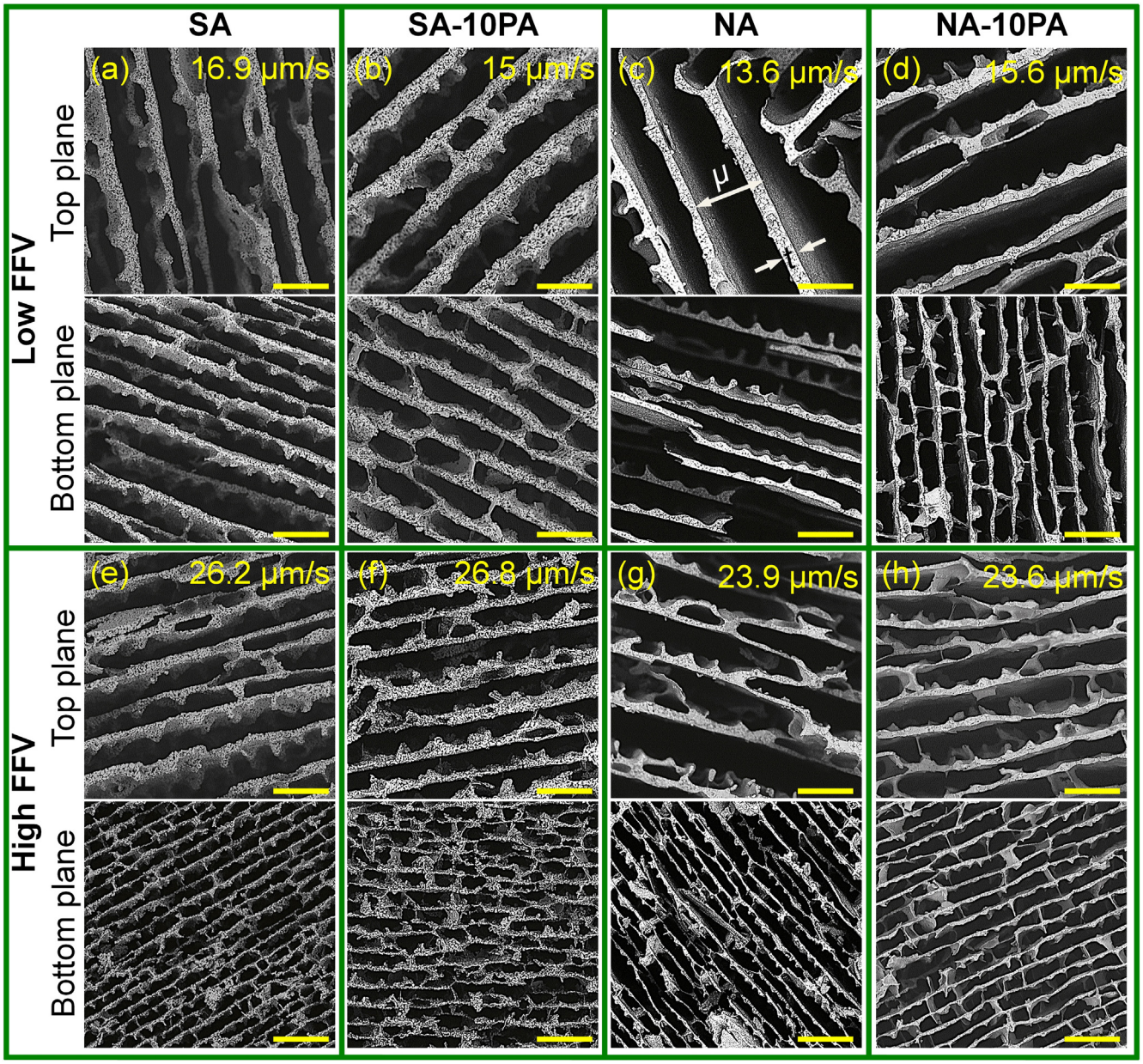


**Fig. 1.** SEM micrographs of the top and bottom planes of the ice-templated porous $Al_2O_3$ scaffolds processed at relatively low and high freezing front velocities (FFVs). Ice growth direction is out of the page and length of the scale bar is 30 μm.

to the SA and NA, respectively. However, the interlamellae bridging is observed to be negligible on the top planes at low FFVs for all the scaffolds compositions. Overall, it can be stated that the bridge density decreased progressively along the ice growth direction (bottom to top). Although not measured but qualitatively for a given composition and FFV, lamella thickness ($t$) and wavelength ($\mu$) increased gradually along the ice growth direction (Fig. 1). The observed progressive microstructural variations along the ice growth direction are typical of the ice-templated scaffolds and are attributed to the difficulty of maintaining a constant FFV over long distance (cm) [2,4,6–8]. Note that the distance in between the bottom and top planes is 2.5 cm (Fig. S1b). Microstructural investigation of all the scaffold compositions at all the FFVs is beyond the scope of this manuscript; however, Fig. 1 indicates that for a given composition the lamellae bridge density increased gradually with the FFV.

Microstructural observations made from Fig. 1 for the SA-10PA and NA-10PA porous scaffolds suggest a governing role of the $Al_2O_3$ platelets in the interlamellae bridge formation. For the SA-10PA (Fig. 2a), platelets are readily visible in between the lamellae (referred to as interlamella platelets, indicated by green arrows) and within the lamella walls (referred to as intralamella platelets, indicated by yellow arrows). Although most of the intralamella and interlamella platelets are observed to be mutually perpendicular, overall they are orientated in the direction of the ice growth. For both the SA-10PA (Fig. 2a) and NA-10PA (Fig. 2b) scaffolds, the interlamella platelets are observed to form majority of the bridges and a single platelet directly connects the adjacent lamellae for most of the bridges. Growth of the ice crystals during the unidirectional freezing can self-assemble large anisotropic particles and orient those particles along the crystal growth direction [9,10]. Thus, during unidirectional freezing some of the $Al_2O_3$ platelets ejected by the advancing ice fronts accumulated in between the ice lamellae and were aligned by the growing ice crystals. As a result, the intralamella platelets are observed to be almost parallel to the lamella walls. On the other hand, lamellae bridges that formed through the interlamella platelets possibly resulted by a different mechanism. As the advancing ice crystals encountered with the $Al_2O_3$ platelets, some